AD-A060 149 RENSSELAER POLYTECHNIC INST TROY N Y DEPT OF MECHANI--ETC F/G 11/6
UNIAXIAL VISCOPLASTICITY BASED ON TOTAL STRAIN AND OVERSTRESS.(U)
JUL 78 M C LIU, E KREMPL N00014-76-C-0231
UNCLASSIFIED RPI-CS-78-4 NL

END
DATE FILMED
12-78
DDC

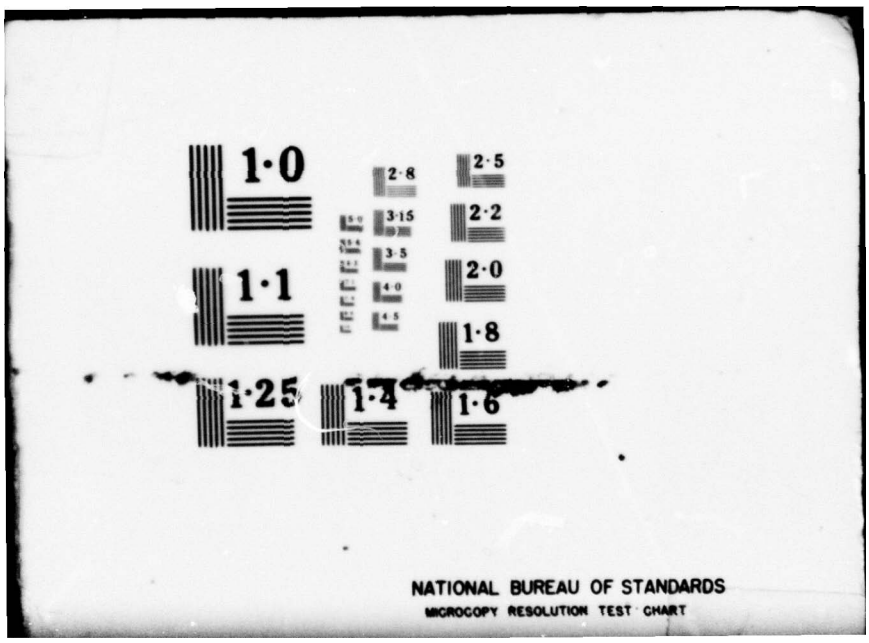
1·0
1·1
1·25
2·8
3·15
3·5
4·0
4·5
1·4
2·5
2·2
2·0
1·8
1·6
NATIONAL BUREAU OF STANDARDS
MICROCOPY RESOLUTION TEST CHART

AD A060149

DDC FILE COPY

LEVEL II

(12)

DDC
RECEIVED
OCT 23 1978
D

DISTRIBUTION STATEMENT A
Approved for public release;
Distribution Unlimited

ACCESSION for
NTIS White Section
DDC Buff Section
UNANNOUNCED
JUSTIFICATION
BY
DISTRIBUTION/AVAILABILITY CODES
Dist. AVAIL. and/or SPECIAL
A

LEVEL II

12

See back page for 1473

UNIAXIAL VISCOPLASTICITY BASED ON TOTAL STRAIN AND OVERSTRESS

M.C.M. Liu and E. Krempl
Department of Mechanical Engineering,
Aeronautical Engineering & Mechanics
Rensselaer Polytechnic Institute
Troy, New York 12181

AD A060149

Report No. RPI CS 78-4

July 1978

DDC FILE COPY

DDC
RECEIVED
OCT 23 1978
D

DISTRIBUTION STATEMENT A
Approved for public release;
Distribution Unlimited

78 10 17 062

UNIAXIAL VISCOPLASTICITY BASED ON TOTAL STRAIN AND OVERSTRESS

M.C.M. Liu and E. Krempl
Department of Mechanical Engineering,
Aeronautical Engineering & Mechanics
Rensselaer Polytechnic Institute
Troy, New York 12181

ABSTRACT

A previously proposed uniaxial constitutive equation nonlinear in the Cauchy stress and the engineering strain but linear in the stress and strain rates is specialized to an overstress model. Two unknown coefficient functions are determined by extrapolation of room temperature relaxation data on Type 304 stainless steel. The stiff first-order nonlinear differential equations are then numerically integrated for a variety of test histories. These include: strain control with strain rates from 10^{-6} s^{-1} to 500 s^{-1}; stress control with stress rates from 1.95 KPa s^{-1} to 19.5 MPa s^{-1}; instantaneous large changes in strain rate (strain-rate history effects) and stress rate; partial unloading and reloading in strain and stress control and tension-tension cyclic creep. The computed results show good qualitative agreement with tests. Based on these results we consider the model a good representation of metal deformation behavior as long as the overstress does not change sign.

Introduction

In previous papers we investigated qualitatively the behavior of a constitutive equation linear in the stress rate and the strain rate tensors but nonlinear in the stress and the strain tensor, Cernocky and Krempl (1978a and 1978b). The constitutive equation considered is basically that of a nonlinear viscoelastic solid. A view advanced by Krempl (1975) asserts that viscoplasticity phenomena can be represented by piecewise nonlinear viscoelasticity. To account for the effects of deformation-induced microstructural changes a discontinuous updating of the material parameters and the introduction of new origins are necessary, Krempl (1975).

The proposed approach does not decompose the strains a priori and considers rate (time)-independence as a limiting form of rate (time)-dependence. It has long been a feature of "dynamic plasticity", Cristescu (1967), Campbell and Dowling (1970), Frantz and Duffy (1972), Nicholas (1971), Klepaczko (1973), Eleiche and Campbell (1976), and of materials science orientated papers, Lubahn (1961), Hart et al. (1975), Miller (1976), Swearengen and Rohde (1977). Also in "static plasticity" rate dependence has been considered recently, Eisenberg et al. (1977), Bodner and Partom (1975) and Guelin and Stutz (1977). The above listing, while incomplete, indicates that rate dependence is gaining increasing attention.

The present approach does not use a yield surface and the transition from linear to elastic to nonlinear inelastic behavior is smooth. Total strain appears explicitly in the equations and the concept of an equilibrium stress-strain curve is used, Walker (1976), Eisenberg et al. (1977), Walker and Krempl (1978).

The purpose of the present paper is to specialize the previously proposed constitutive equation to an overstress model and to compute the two material functions of the theory from relaxation tests on Type 304 stainless steel at

room temperature, Yamada and Li (1973). Then the predictive capability of the equation is tested by numerically integrating the resulting stiff nonlinear differential equation for a variety of test histories which include tensile tests under strain and stress control which involve several orders of magnitudes in the rates; instantaneous large changes in the rates, creep followed by tensile loading; unloading and reloading under stress and strain control; and cyclic creep ratcheting. The results show qualitative agreement with experiments, Krempl (1978) (no quantitative fit is attempted at this time). All the numerical tests are performed such that the overstress does not change sign. Should this occur modifications to the model are necessary; these will be treated in a forthcoming paper.

The Proposed Constitutive Equation

The uniaxial form of a previously proposed constitutive equation, Cernocky and Krempl (1978a, 1978b), when specialized to an overstress model is

$$m[\sigma - g[\varepsilon]]\dot{\varepsilon} + g[\varepsilon] = \sigma + k[\sigma - g[\varepsilon]]\dot{\sigma} . \tag{1}$$

In the above, square brackets denote a function of the enclosed quantity, ε is the engineering total strain and $\dot{\varepsilon}$ its time derivative. The Cauchy (true) stress is σ and $\dot{\sigma}$ is its time derivative. The functions $m[\cdot]$ and $k[\cdot]$ are bounded, positive and even; for all values of their arguments they are related by

$$\frac{m[\cdot]}{k[\cdot]} = E \tag{2}$$

where E is the elastic modulus. The function $g[\varepsilon]$ is odd. With these requirements compression and tension responses are symmetric with respect to the origin.

It is shown by Cernocky and Krempl (1978a) that (1) and (2) together with the above conditions on the functions ensure the following properties:

- Initial linear elastic behavior for all rates of loading
- Linear elastic behavior in the limit for very fast loading
- For very slow loading $\sigma = g[\varepsilon]$; $g[\varepsilon]$ is therefore the "equilibrium stress-strain curve", Walker (1976), Eisenberg et al. (1977)
- Elastic slope upon large instantaneous changes in strain (stress) rate in the plastic range
- In the plastic range a stress-strain curve at a given rate of loading will be equidistant to $g[\varepsilon]$
- Stress-strain curves obtained at different rates of loading are nonlinearly spaced
- A creep test for positive creep stress has $\dot{\varepsilon} \geq 0$, $\ddot{\varepsilon} \leq 0$ provided $g'[\varepsilon] \geq 0$. Primary and secondary creep may be reproduced.
- For positive strain $\dot{\sigma} \leq 0$, $\ddot{\sigma} \geq 0$ in a relaxation test. Relaxation terminates at $\sigma = g[\varepsilon]$.

Further details may be found in Cernocky and Krempl (1978a).

It is shown by Cernocky and Krempl (1978a) that for tests with constant strain rate α the following expressions hold for large strains:

$$\frac{d\sigma}{d\varepsilon} = g'[\varepsilon] \tag{3}$$

and

$$\{\sigma - g[\varepsilon]\} = (E - g'[\varepsilon])k[\sigma - g[\varepsilon]]\alpha. \quad ^{1)} \tag{4}$$

The above equations are valid in the plastic range where $g'[\varepsilon] \ll E$. Equation (4) then shows that in the plastic range $\{\sigma - g[\varepsilon]\} \approx$ constant[2)] and substantiates the fifth statement listed above. We denote this limiting value as $\{\sigma - g[\varepsilon]\}$.

---

1) Mathematically (3) and (4) are limits obtained for large strains ($\varepsilon \to \infty$). These limits are, however, rapidly obtained, see Cernocky and Krempl (1978a).

2) If $g'[\varepsilon]$ = constant beyond some strain then $\{\sigma - g[\varepsilon]\}$ can be constant. In reality $g'[\varepsilon] \ll E$ so that small variations in $g'[\varepsilon]$ are of minor influence on the value of $\{\sigma - g[\varepsilon]\}$.

Relaxation and Constant Strain Rate Tests

Specialization of Eq. (1) for the relaxation test yields

$$\dot{\sigma} = \frac{g[\epsilon_o] - \sigma}{k[\sigma - g[\epsilon_o]]} \tag{5}$$

which has to be solved for a suitable initial condition, say $\sigma = \sigma_o$ at $t = t_o$, to obtain the relaxation curve.

From room temperature relaxation experiments on some metals started from a point in the plastic range of the stress-strain curve, the following was observed:

A) For a given time interval the amount of stress relaxation depends only on the strain rate[3] of the stress-strain curve preceding the relaxation test, Krempl (1978).

B) The initial inelastic strain rate $|\dot{\sigma}/E|$ in a relaxation test is independent of the initial stress and strain value and equal to the strain rate of the tensile test preceding the relaxation test, Yamada and Li (1973), Thomas and Yaggee (1975), Hart et al. (1975).

C) Graphs of σ vs $|\dot{\sigma}/E|$ of a set of relaxation tests started at various strains in the plastic range, say ϵ_n, $n = 0, 1, 2, 3 \ldots$ share a common appearance, Yamada and Li (1973), Thomas and Yaggee (1975), Hart et al. (1975). Figure 1 shows an example of the relaxation curves obtained by Yamada and Li (1973) on Type 304 stainless steel at room temperature.

Below we show that (1) can reproduce these observations.

From (4) we see that for a suitable function $k[\cdot]$, the value of $\{\sigma - g[\epsilon]\}$ is uniquely related to the strain rate and that $\{\sigma - g[\epsilon]\}$ is approximately constant in the plastic range, see also, Cernocky and Krempl (1978a). Suppose now that a relaxation test is started after some constant strain rate test during which some $\{\sigma - g[\epsilon]\}$ is reached. For the relaxation test we

---

[3] Unless stated otherwise strain and strain rate designate total strain and total strain rate, respectively.

obtain from (5) after separation of variables and using $y = \sigma - g[\epsilon_n]$ with ϵ_n, $n = 0, 1, 2 \ldots$ designating different constant strains in different relaxation tests

$$t - t_o = - \int_{\sigma_n - g[\epsilon_n]}^{\sigma - g[\epsilon_n]} \frac{dy\, k[y]}{y} \tag{6}$$

where σ_n is the initial stress.

Since $\sigma_n - g[\epsilon_n] = \{\sigma - g[\epsilon]\}$ = constant by (4), the lower limit of the integral in (6) is equal for all tests considered in this example. Integration of (6) yields

$$t - t_o = A[\sigma - g[\epsilon_n]] - A[\sigma_n - g[\epsilon_n]] \tag{7}$$

where $A[\cdot]$ is the indefinite integral of (6). We consider two tests started at ϵ_1 and ϵ_2 which reach at the same $t_1 - t_o = \Delta t = t_2 - t_o$ the stress $\hat{\sigma}$ and $\hat{\hat{\sigma}}$, respectively. Then from (7) and since $\sigma_1 - g[\epsilon_1] = \sigma_2 - g[\epsilon_2]$

$$A[\hat{\sigma} - g[\epsilon_1]] = A[\hat{\hat{\sigma}} - g[\epsilon_2]]. \tag{8}$$

If $A[\cdot]$ is bijective (which in return restricts $k[\cdot]$) we conclude that the arguments in (8) are equal and therefore

$$\{\hat{\sigma} - \sigma_1\}_{\Delta t} = \{\hat{\hat{\sigma}} - \sigma_2\}_{\Delta t} . \tag{9}$$

Equation (9) together with (4) shows that (1) can reproduce A) mentioned previously.

It should be stressed that only the $\sigma - g[\epsilon]$-dependence of $k[\cdot]$ can reproduce both A) and the nonlinear spacing of stress-strain curves obtained at various loading rates, see Cernocky and Krempl (1978a).

To show that B) is within the predictive capability of (1) we rewrite (1) using (2) as

$$\dot{\epsilon} = \dot{\sigma}/E + \frac{\sigma - g[\epsilon]}{Ek[\sigma - g[\epsilon]]} \tag{10}$$

or

$$\dot{\epsilon} = \dot{\epsilon}_{el} + \dot{\epsilon}_{in} \,. \tag{11}$$

For $\sigma - g[\epsilon]$ = constant the inelastic strain rate is constant. It is equal to the <u>initial</u> inelastic relaxation rate $|\dot{\sigma}/E|$ in a relaxation test, see Eq. (5). Using the chain rule (10) can be rewritten as

$$\dot{\epsilon}\left(1 - \frac{1}{E}\frac{d\sigma}{d\epsilon}\right) = \frac{\sigma - g[\epsilon]}{Ek[\sigma - g[\epsilon]]} \tag{12}$$

and since $\frac{1}{E}\frac{d\sigma}{d\epsilon} \ll 1$ in the plastic range $\dot{\epsilon} \approx \dot{\epsilon}_{in}$. Our equation predicts B).

Consider a relaxation test with constant strain ϵ_o, then from (5)

$$\{-\dot{\sigma}/E\}_{\epsilon_o} = \{\dot{\epsilon}_{in}\}_{\epsilon_o} = \frac{\sigma - g[\epsilon_o]}{k[\sigma - g[\epsilon_o]]E} \equiv f[\sigma] \tag{13}$$

where in writing $f[\sigma]$ we have suppressed the parametric dependence on ϵ_o. Consider any other relaxation test started at some ϵ_n, then from (7) and (13)

$$\{-\dot{\sigma}/E\}_{\epsilon_n} = \{\dot{\epsilon}_{in}\}_{\epsilon_n} = \frac{\sigma - g[\epsilon_o] - \{g[\epsilon_n] - g[\epsilon_o]\}}{k[\sigma - g[\epsilon_o] - \{g[\epsilon_n] - g[\epsilon_o]\}]E} = f[Y] \tag{14}$$

with $Y = \sigma - \{g[\epsilon_n] - g[\epsilon_o]\}$. Equation (14) says that a translation by $\{g[\epsilon_n] - g[\epsilon_o]\}$ will make the inelastic strain rate vs. stress curves for the test with ϵ_o and the test with ϵ_n coincident.

With regard to Fig.1, this means that a replot of the curves using a <u>linear</u> stress scale should permit a translation along the σ-axis of all the curves to form one single curve. (The function $f[\cdot]$ postulated in (13) is of course the one plotted in Fig.1.)

We have examined the room temperature relaxation curves reported by Yamada and Li (1973), Thomas and Yaggee (1975) and Hart et al. (1975) and have found that the translation is possible within the experimental accuracy stated by the authors. We consider this fact another confirmation of the validity of (1) and (2) as a model for metal deformation behavior.

Determination of $g[\epsilon]$ and $k[\sigma - g[\epsilon]]$ from Relaxation Tests

To determine the two unknown material functions in (1) we used the data shown in Fig.1 taken from Yamada and Li (1973). Equation (5) predicts that relaxation terminates when $\sigma = g[\epsilon_o]$. At this point from (5)

$$\left\{\frac{d\sigma}{d \log |\dot{\sigma}|}\right\}_{\sigma=g[\epsilon_o]} = 0 . \tag{15}$$

The curves in Fig.1 do not show a horizontal tangent and therefore they were extrapolated to find three points of the $g[\epsilon]$ curve for which (15) is valid. (Presumably the tests were terminated before this condition was reached; a test reported by Swearengen and Rohde (1977) exhibits condition (15).) Then a function developed by Liu et al. (1976) was used to approximate $g[\epsilon]$. The chosen $g[\epsilon]$, together with the data points (circles), are shown in Fig.2. Using the results displayed in Fig.1, the $g[\epsilon]$ shown in Fig.2 and Eq.(5), it is possible to calculate $k[\sigma - g[\epsilon]]$. The results are shown in Fig.3.

A careful analysis of the data in Fig.3, together with general requirements on the properties of the k-function, see Cernocky and Krempl (1978a), suggest that $k[\cdot]$ can be approximated by a double exponential function of the form

$$k[x] = R_o \exp\{R_1 \exp - R_2 |x|^{R_3}\} \tag{16}$$

where R_o through R_3 are suitable positive constants.

The functions k_1 and k_3 in Fig.3 were selected so that they approximate the material data where such data are available. They are both extended beyond the range of available data. A separate function k_2 is also shown in Fig.3 which is unrelated to the others.

Considering the graphs of the k-functions in Fig.3, we see that $\frac{dk[x]}{dx} \leq 0$ always. For these functions Eq.(4) yields a unique value of $\{\sigma - g[\varepsilon]\}$ for a given α and the conclusions following Eq.(7) hold true. Therefore the functions k_1, k_2 and k_3 in Fig.3 are suitable for our purposes.

By the above procedure we have found the two material functions in (1) and have therefore completely characterized the constitutive equation. We are therefore in a position to test the predictive capability of (1) under various input histories. It should be recalled that (1) is considered a valid model for metals only as long as $\sigma - g[\varepsilon]$ does not change sign. In the following we will only consider numerical examples where this condition is satisfied.

Numerical Experiments

For a given input stress or strain history, (1) is a nonautonomous, stiff, first-order nonlinear differential equation. For the numerical solution of this equation we used an algorithm with automatic step size adjustment developed by Bulrisch and Stoer (1966). The computations were carried out on an IBM 360/67 computer and the results were graphed using a Calcomp plotter. Unless stated otherwise the $g[\varepsilon]$-function shown in Fig.2 and the k_1-function shown in Fig.3 are used in the computation.

Monotonic Loading at Different Loading Rates

Stress-strain curves for strain rates between 10^{-6} and 10^{-1} s^{-1} and for stress rates between .283 psi/s to 2830 psi/s (1.95 kPa s^{-1} - 19.5 MPa s^{-1}) are shown in Figs.2 and 4, respectively. The curves are nonlinearly spaced as predicted by the theory of Cernocky and Krempl (1978a).

Initially when the curves at various loading rates coincide with $g[\varepsilon]$ our model behaves as a linear elastic material. Then the spacing between a stress-strain curve and $g[\varepsilon]$ increases and inelastic behavior starts to develop gradually. In the nearly linear portions of the stress-strain diagram creep and relaxation are small and the rates of creep and relaxation are extremely low. This behavior corresponds to the one observed by Krempl (1978) in Figs.4 and 6, which show that the transition from elastic to inelastic behavior is gradual.

The k_1-function shown in Fig.3 is constant beyond a certain value of $\sigma - g[\varepsilon]$. As a consequence the spacing of the stress-strain curves will become proportional to the strain rate above a certain strain rate. At high strain rates (500 s^{-1}) the curves would follow the elastic line in Fig.2.

Experiments on cold-worked 304 SS, Albertini and Montagnani (1976 and 1977), show that stress-strain curves obtained at strain rates near 10^{+3} s^{-1} are not linear elastic.

To accommodate such a behavior it is necessary to have a k-function that extends to smaller k-values than the k_1-function used so far. The k_3-function fulfills this requirement. Stress-strain curves at 10^{-2} and 5×10^{2} s^{-1} are computed with k_3 and displayed in Fig.5. Since k_1 and k_3 are initially identical the 10^{-2} s^{-1} curves in Figs.2 and 5 are equal. The 500 s^{-1} curve would, however, be a straight line in Fig.2 if k_1 was used.

Examination of Figs.2 and 3 shows that the k_1- and the k_3-function should give identical results for all tests for which $|\sigma - g[\varepsilon]| \leq 12$ ksi, i.e., for strain rates less than 10^{-2} s^{-1} or stress rates below 2.83 ksi s^{-1} (19.5 MPa s^{-1}). However, k_3 insures reasonable results for high loading rates.

It is of interest to observe that the initial stresses of the relaxation tests reported by Yamada and Li (1973) and shown in Fig.1 fall on the stress-strain curve for a strain rate of 10^{-4} s^{-1}, see the x-marks in Fig.2.

Equation (1) can also represent nearly rate-independent behavior, Cernocky and Krempl (1978a). To demonstrate this we have constructed the function k_2 in Fig.3 and have computed the resulting stress-strain curves for stress control shown in Fig.6. The curves are much closer together in Fig.6 than in Fig.4 (the same stress rates and the same $g[\varepsilon]$ apply in both cases) indicative of the reduced rate sensitivity of this hypothetical material.

Sudden Changes in Strain Rate or Stress Rate

Using the chain rule, Eqs. (1) and (2) can be rewritten as

$$\frac{d\sigma}{d\varepsilon} = E - \frac{\sigma - g[\varepsilon]}{k[\cdot]\dot{\varepsilon}} \tag{17}$$

or as

$$\frac{d\varepsilon}{d\sigma} = \frac{1}{E} + \frac{\sigma - g[\varepsilon]}{Ek[\cdot]\dot{\sigma}} \tag{18}$$

where the first is suitable for "strain control" and the second for "stress control".

Let the strain (stress) rate be changed from $\dot{\varepsilon}^-$ to $\dot{\varepsilon}^+$ ($\dot{\sigma}^-$ to $\dot{\sigma}^+$) and let $\frac{d\sigma^-}{d\varepsilon}$ and $\frac{d\sigma^+}{d\varepsilon}$ be the slope of the stress-strain diagram immediately before and after the discontinuous change in loading rate, respectively. Then from (17) and (18)

$$\frac{d\sigma^+}{d\varepsilon} = E\left(1 + \left(\frac{\frac{d\sigma^-}{d\varepsilon}}{E} - 1\right)\frac{1}{a}\right) \tag{19}$$

and

$$\frac{d\sigma^+}{d\varepsilon} = E\left(1 + \frac{1}{b}\left(\frac{E}{\frac{d\sigma^-}{d\varepsilon}} - 1\right)\right)^{-1}, \tag{20}$$

respectively. In the above $a = \frac{\dot{\varepsilon}^+}{\dot{\varepsilon}^-}$ and $b = \frac{\dot{\sigma}^+}{\dot{\sigma}^-}$. A sketch of (19) and (20) is given in Figs.7a and 7b, respectively.

It is interesting to observe that for a rate increase ($a > 1$ or $b > 1$) the subsequent slope approaches E in both cases. For a rate decrease ($0 \leq a < 1$, $0 \leq b < 1$) the slope decreases to zero for the stress controlled case but reaches negative infinity in the strain controlled case. For rate reversal ($a < 0$; $b < 0$) the slope is always larger than E in the strain controlled case whereas negative and positive values of the slope are possible for stress control. If $\frac{d\sigma^-}{d\varepsilon} \approx E$ then $\frac{d\sigma^+}{d\varepsilon} \approx E$ irrespective of the value of a or b.

The results of numerical experiments demonstrating this difference are shown in Figs.8a, 8b and 9a and 9b, respectively.

In Fig.8, the unloading and reloading behavior under strain control, Fig.8a, and stress control, Fig.8b, are shown. When $\sigma = g[\varepsilon]$ we reload and continue the numerical test to 2% strain. The differences in strain and stress control are obvious, as well as is the elastic slope as the curve $g[\varepsilon]$ is approached.

The loading rates are cycled between two limits in Figs.9a (strain control) and Fig.9b (stress control). The curves demonstrate visually the difference in the behavior predicted by (19) and (20). Experiments reported in Fig.10 of Krempl (1978) correspond qualitatively to the behavior depicted in Fig.9a.

Cyclic Creep and Creep Hardening

In Fig.10a we have computed the behavior of our model under stress controlled cyclic loading using the stress rates indicated on the figure. Note that at point A the stress rate was reversed and reduces tenfold and the slope after point A is shallow and negative as given by (20). The amount of "creep strain" accumulated during each cycle reduces with cycles, compare the distances BD, DF .... JL. Figure 9 of Krempl (1978) shows that 304 stainless steel exhibits this behavior in uniaxial tests. The quantity E_T is the tangent modulus of $g[\varepsilon]$ in the plastic range ($g[\varepsilon]$ is not plotted in this case). In Fig.10b E_T is reduced by about 1/3 with a considerable effect on the accumulated creep strain. After completion of the first reloading BC the arbitrarily imposed strain limit of 2% was reached.

Figures 11a and 11b show the creep behavior followed by tensile loading. In going from Fig.11a to Fig.11b only the creep time was changed from .015 hrs to 1 hr. It is evident that the initial slope at B increased with increasing creep time. This observation is sometimes referred to as creep hardening, and is also interpreted as creep-plasticity interaction, see Figs.6 and 8 in Pugh and Robinson (1978).

The phenomena shown in Fig.10 (reduction of accumulated creep strain with increasing cycles) and Fig.11 (creep hardening) are reproduced by our viscoelastic solid, Eq.(1). The reason for this capability lies in the $\sigma - g[\varepsilon]$-dependence of the equation and the dependence of k on $\sigma - g[\varepsilon]$ as shown in Fig.3.

We see from Eqs.(17) and (18) that the slope $\frac{d\sigma}{d\varepsilon}$ approaches E as $\sigma - g[\varepsilon] \to 0$. This limit is approached rapidly since k increases strongly with decreasing argument, see Fig.3.

In the creep tests with positive stress the strain is increasing and the strain point moves towards smaller values of $\sigma_o - g[\varepsilon]$. The present model predicts, see (17) and (18), that the initial slope of a subsequent stress-strain curve will be approaching E as the creep strain increases. It is therefore capable of representing creep-hardening by virtue of the $\sigma - g[\varepsilon]$-dependence of the equation.

Discussion

The numerical experiments reported herein and the previous qualitative discussions of the model by Cernocky and Krempl (1978a) show that (1) has very attractive features as a model of metal deformation behavior. Comparison with experiments, Krempl (1978), demonstrates qualitative correspondence between actual material behavior and test results for room temperature.

In addition to the qualitative features mentioned previously the model presented herein can in principle reproduce the observations reported in Fig.11 of Krempl (1978). In this figure the results of one relaxation test [the stress vs. the inelastic strain rate defined in (13)] and the results of strain rate change test (stress change $\Delta\Sigma$ vs. strain rate assuming that one point is on the relaxation curve) fall on one curve. To show that the theory presented herein can reproduce this observation we assume that the relaxation curve $\dot{\varepsilon}_{in}$ vs σ is given by Eq. (13). In the "plastic range", the strain rates $\dot{\varepsilon}_1$ and $\dot{\varepsilon}_2$ in two tensile tests are given by, see (12)

$$\dot{\varepsilon}_1 \approx \frac{\sigma_1 - g[\varepsilon_1]}{Ek[\sigma_1 - g[\varepsilon_1]]} \equiv f[\sigma_1] \tag{21}$$

and

$$\dot{\varepsilon}_2 \approx \frac{\sigma_2 - g[\varepsilon_2]}{Ek[\sigma_2 - g[\varepsilon_2]]} \tag{22}$$

where $\varepsilon_2 = \varepsilon_1$ since the stresses σ_1 and σ_2 are measured at the same strain, see Fig.3 of Krempl (1978).

Let $\sigma_2 = \Delta\sigma + \sigma_1$, then from (22)

$$\dot{\varepsilon}_2 = \frac{\Delta\sigma + \sigma_1 - g[\varepsilon_1]}{Ek[\Delta\sigma + \sigma_1 - g[\varepsilon_1]]} = f[\sigma_1 + \Delta\sigma] \ . \tag{23}$$

Now if (21) is made to coincide with the relaxation curve in Fig.11 of Krempl (1978), the translation $\{g[\varepsilon_1] - g[\varepsilon_o]\}$, see Eq.(14), is necessary. From (22) and (23) we deduce that the point $\dot{\varepsilon}_2$ must be found on the relaxation curve $\Delta\sigma$ units away from σ_1. This is exactly the evidence found in Fig.11 of Krempl (1978).

The differences in the unloading behavior in "stress-" and "strain-control" displayed in Figs.7 through 10 are reminiscent of the behavior obtained in a 'soft" and "stiff" testing machine, respectively. Of course, servocontrolled testing has eliminated the need for such a distinction.

The $\sigma - g[\varepsilon]$ dependence of (1) renders this equation in essence an overstress model, Malvern (1951), Perzyna (1963). This particular feature is of great importance in modelling viscoplastic behavior as discussed previously. We note that the yield surface and the decomposition of the strain into elastic and inelastic parts is not used in our approach.

The function $g[\varepsilon]$ could be considered the equilibrium stress-strain curve of Walker (1976) and Eisenberg et al. (1977) and for a given ε, $g[\varepsilon]$ could be interpreted as the rest-stress, a concept used by Rice (1970) and Miller (1976). In their approach the inelastic strain rate is zero when the applied stress reaches the rest stress. This property is shared by the present model.

Equation (1) is basically an equation of state, i.e., knowledge of any three variables of σ, $\dot{\sigma}$, $\dot{\epsilon}$ and ϵ determines the fourth uniquely. No internal variables are used. Generally one might therefore be inclined to dismiss Eq. (1) which was shown to exhibit very desirable properties. It has to be recognized that any mathematical representation is only a model of the real material which macroscopically represents behavior which is the result of many micromechanisms. The precise way in which the many microstructural mechamisms combine to a macroscopic response is not known. Even in the micromechanical or internal variable theories the macroscopic effects of micromechanisms can only be ascertained by determining constants or functions from measurements of macroscopic stress and strain. Since our functions are obtainable from such measurements they represent the microstructure of the material in a phenomenological way. Specifically $g[\epsilon]$ could be considered the repository for strain (work) hardening.

The model given in Eq. (1) is considered to be valid for metals at low homologous temperature as long as $\sigma - g[\epsilon]$ does not change sign. If unloading would proceed beyond $\sigma \approx g[\epsilon]$ then we modify the equation through introduction of new origins and updating the function constants, see Liu et al. (1976) for the rate-independent case. This extension of the present model will be published elsewhere. The updating of the function constants is a recognition of the fact that the real material has changed its microstructure due to the loading up to the point $\sigma - g[\epsilon] = 0$. (Up to the point $\sigma - g[\epsilon] = 0$ the microstructural effects are included in the material functions $k[\cdot]$ and $g[\cdot]$.)

The model is suitable for static as well as dynamic plasticity. In the latter case the prediction strain-rate history effect is included in its capability.

Acknowledgement

This work was sponsored by the National Science Foundation and the Office of Naval Research. It is a pleasure to acknowledge helpful discussions with E.P. Cernocky and Dr. H. Moon. We are indebted to Professor H.A. Scarton for making a computer program, based on the paper by Bulrisch and Stoer (1966), available to us.

REFERENCES

Albertini, C., M. Montagnani 1976 Nuclear Eng. and Design 37, 115.

Albertini, C., M. Montagnani 1977 Report EUR 5787.e, Ispra, Italy.

Bodner, S.R., Y. Partom 1975 Trans. ASME, J. Appl. Mech. 42, 385.

Bulrisch, R., J. Stoer 1966 Numerische Mathematik 8, 1.

Campbell, J.D., A.R. Dowling 1970 J. Mech. Phys. Solids 18, 43.

Cernocky, E.P., E. Krempl 1978a RPI Report CS 78-1, to appear in Int. J. Nonlinear Mechanics.

Cernocky, E.P., E. Krempl 1978b RPI Report CS 78-3, to appear in Acta Mechanica.

Eisenberg, M.A., C.W. Lee, A. Phillips 1977 Int. J. Solids and Structures 13, 1239.

Eleiche, A.M., J.D. Campbell 1976 Experimental Mechanics 16, 281.

Frantz, R.A., J. Duffy 1972 Trans. ASME, J. Appl. Mech. 39E, 939.

Guelin, P., P. Stutz 1977 Archives of Mechanics 29, 13.

Hart, E.W., C.Y. Li, H. Yamada, G.L. Wire 1975 MIT Press.

Klepaczko, J. 1975 Mat. Sci. Eng. 18, 121.

Krempl, E. 1975 Acta Mechanica 22, 53.

Krempl, E. 1978 RPI Report CS 78-5.

Liu, M.C.M., E. Krempl, D.C. Nairn 1976 Trans. ASME J. Eng. Matls. and Technology 98, 322.

Lubahn, J.D. 1961 in Mechanical Behavior of Materials at Elevated Temperature, McGraw-Hill, specifically p.325.

Malvern, L.E. 1951 Trans. ASME, J. Appl. Mech. 18E, 269.

Miller, A. 1976 Trans. ASME, J. Eng. Matls. and Technology 98, 97.

Nicholas, T. 1971 Experimental Mechanics 11, 370.

Perzyna, P. 1963 Quart. of Appl. Mech. 20, 321.

Pugh, C.E., D.N. Robinson 1978 Nuclear Eng. and Design 48, 269.

Rice, J.R. 1970 Trans. ASME, J. Appl. Mech. 37E, 728.

Swearengen, J.C., R.W. Rohde 1977 Met. Trans. 8A, 577.

Walker, K.P. 1976 Ph.D. Thesis, Rensselaer Polytechnic Institute.

Walker, K.P., E. Krempl 1978 Mechanics Research Communications, to appear.

Yamada, H., C.Y. Li 1973 Met. Trans. 4, 2133.

FIGURE CAPTIONS

Figure 1 Stress vs. Inelastic Strain Rate Curves Obtained in Relaxation Tests at Various Strains on Type 304 Stainless Steel at Room Temperature, from Yamada and Li (1973)

Figure 2 Computed Stress-Strain Curves at Various Strain Rates. The nonlinear spacing is apparent. The symbols O and X denote extrapolated points and the start of the relaxation tests of Yamada and Li (1973), respectively.

Figure 3 The Various k-Functions used in the Computations. The symbol X denotes data points obtained from the relaxation tests of Yamada and Li (1973).

Figure 4 Computed Stress-Strain Curves at Various Stress Rates

Figure 5 Stress-Strain Curves at Low and Very High Strain Rates Using k_3

Figure 6 Simulated Nearly Rate Insensitive Behavior Using k_2. Compare the spacing of the stress-strain curves with those in Fig. 4.

Figure 7a The Slope of the Stress-Strain Curve Immediately after an Instantaneous Change in Stress Rate, from Eq. (20).

Figure 7b The Slope of the Stress-Strain Curve, Immediately after an Instantaneous Change in Strain Rate, from Eq. (19).

Figure 8a Unloading and Reloading Behavior under Strain Control, $a = -1$

Figure 8b Unloading and Reloading Behavior under Stress Control, $b = -1$

Figure 9a Repeated Instantaneous Changes in Strain Rate in a Tensile Test (Strain-Rate History Effect), $a = 10^2$, $a = 10^{-2}$

Figure 9b Repeated Instantaneous Changes in Stress Rate in a Tensile Test (Stress-Rate History Effect), $b = 10^2$, $b = 10^{-2}$

Figure 10a Cyclic Creep Ratchetting under Tension-Tension Loading. Note the gradual decrease in ratchet strain, compare BD, DF, ... (g[ε1 is not plotted), $b = -10^{-1}$, $b = -1$

Figure 10b — Same as Fig.10a Except that the Plastic Tangent Modulus of $g[\varepsilon]$ has been Decreased by about a Factor of 3.

Note the increase in creep strain, $b = -10^{-1}$, $b = -1$.

Figure 11a — Tensile Test Interripted by a .015 hr Creep Test.
The $g[\varepsilon]$ differs from the one used in the preceding figures.

Figure 11b — Same as Fig.11a Except that the Creep Period has been Increased to 1 hr. The "hardening" of the tensile curve (3 - 4) following the creep test is of interest.

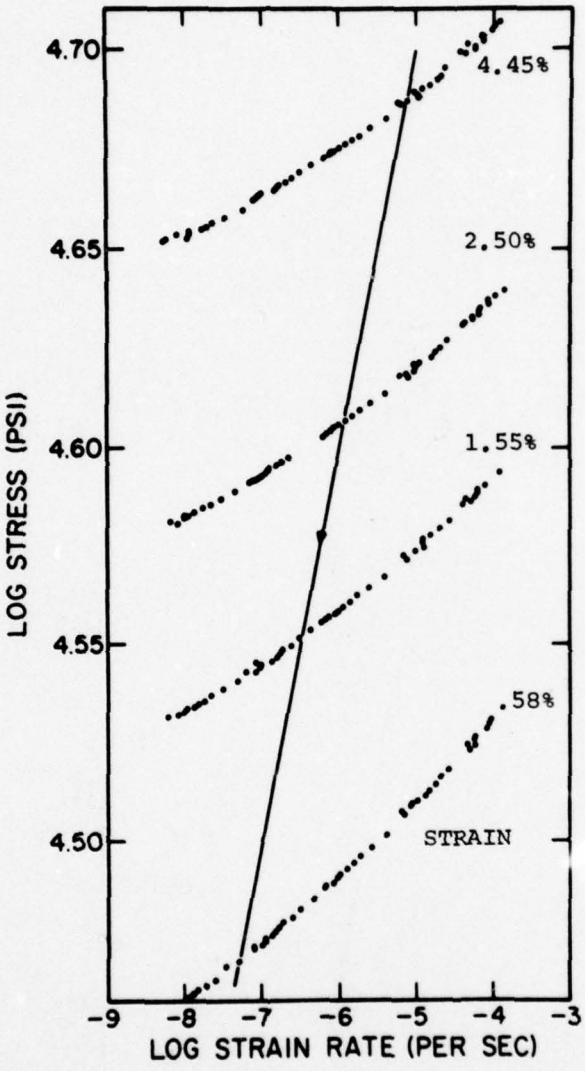
4.70
4.65
4.60
4.55
4.50
LOG STRESS (PSI)
4.45%
2.50%
1.55%
.58%
STRAIN
-9
-8
-7
-6
-5
-4
-3
LOG STRAIN RATE (PER SEC)

FIG.1

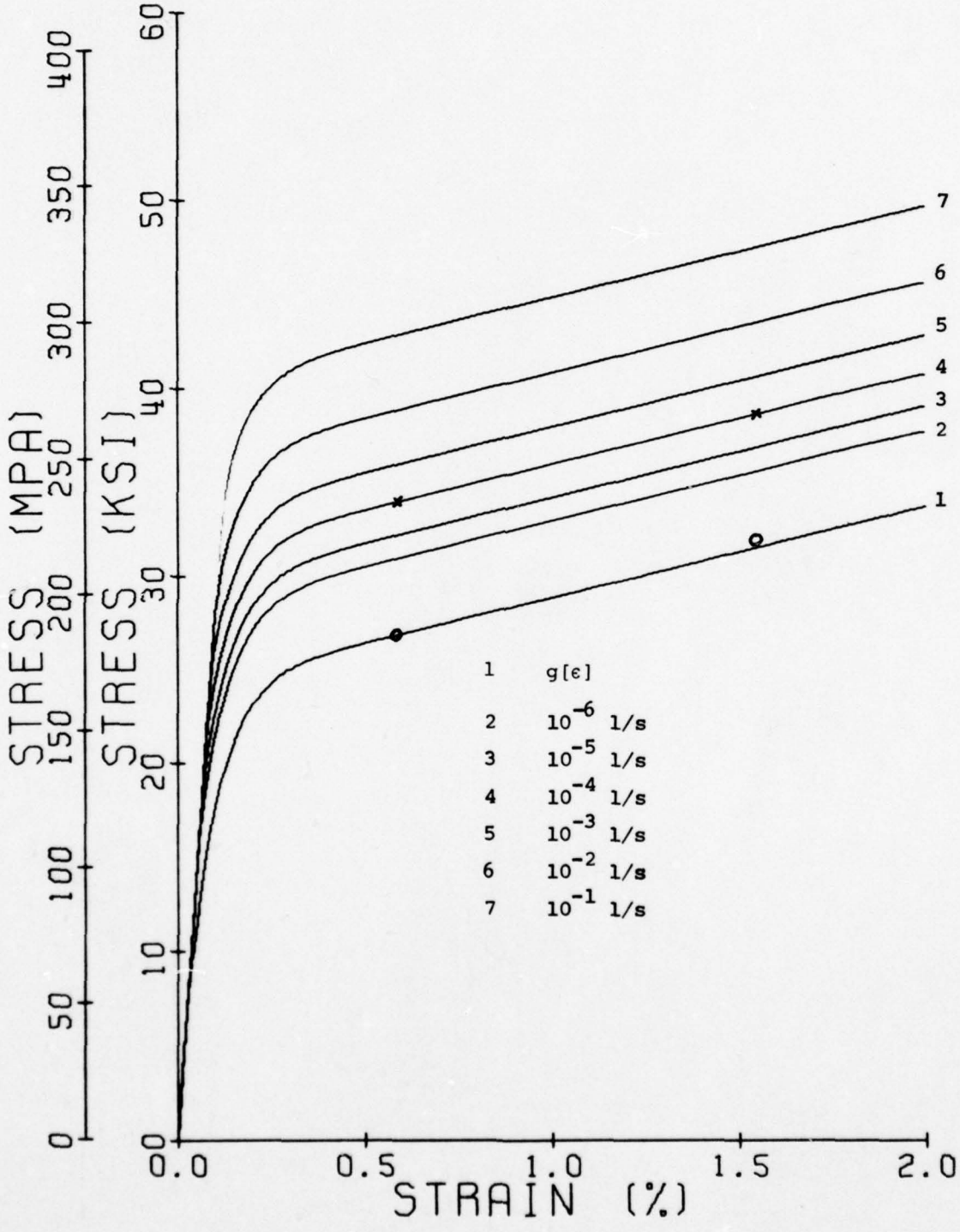
STRESS (MPA)
0
50
100
150
200
250
300
350
400
STRESS (KSI)
0
10
20
30
40
50
60
0.0
0.5
1.0
1.5
2.0
STRAIN (%)
1
2
3
4
5
6
7
1 g[ε]
2 10^-6 1/s
3 10^-5 1/s
4 10^-4 1/s
5 10^-3 1/s
6 10^-2 1/s
7 10^-1 1/s

FIG. 2

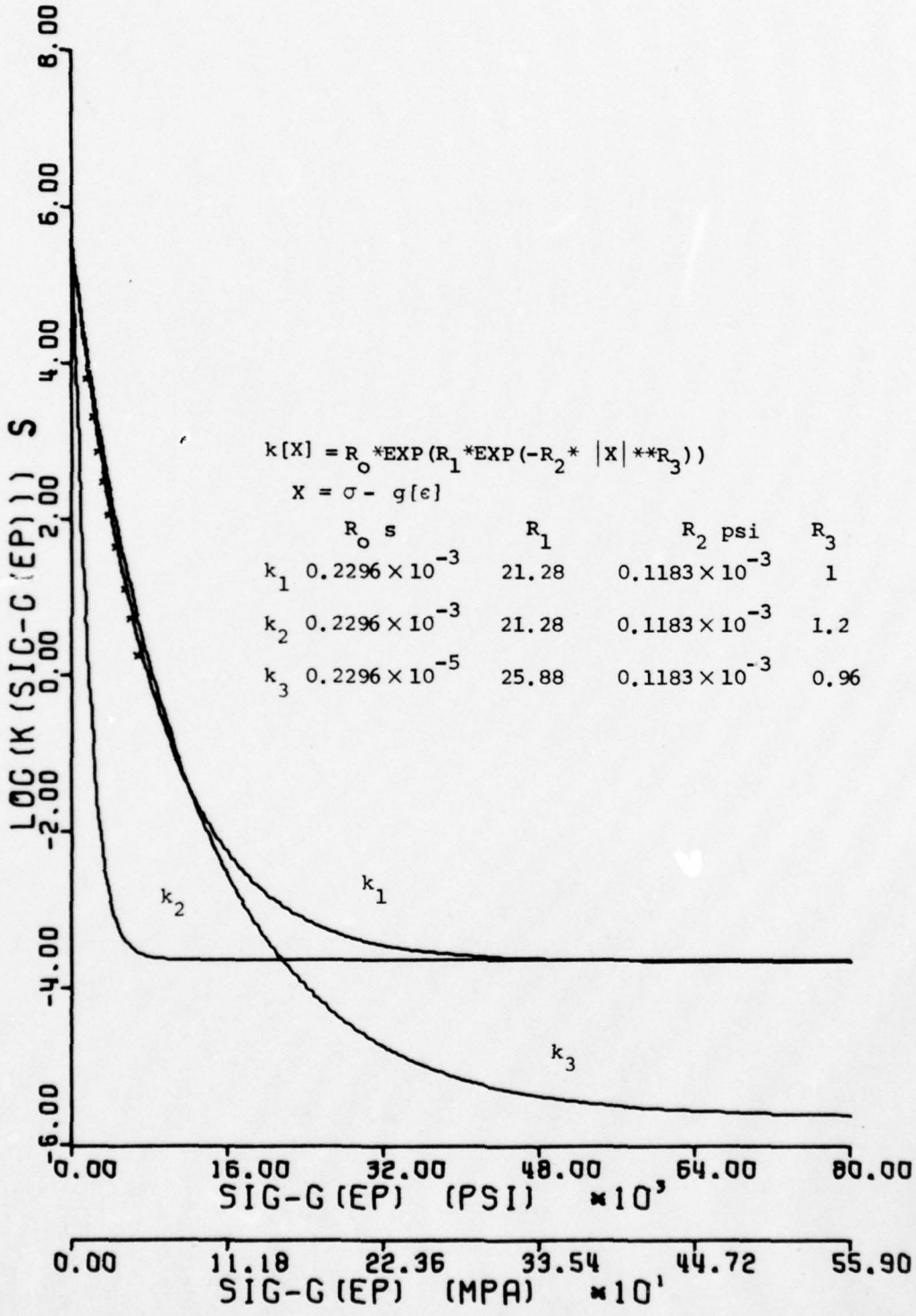
8.00
6.00
4.00
2.00
0.00
-2.00
-4.00
-6.00
LOG(K(SIG-G(EP))) S
k[X] = R_o*EXP(R_1*EXP(-R_2* |X|**R_3))
X = σ - g[ε]
R_o s R_1 R_2 psi R_3
k_1 0.2296 × 10^-3 21.28 0.1183 × 10^-3 1
k_2 0.2296 × 10^-3 21.28 0.1183 × 10^-3 1.2
k_3 0.2296 × 10^-5 25.88 0.1183 × 10^-3 0.96
k_1
k_2
k_3
0.00 16.00 32.00 48.00 64.00 80.00
SIG-G(EP) (PSI) *10^3
0.00 11.18 22.36 33.54 44.72 55.90
SIG-G(EP) (MPA) *10^1

FIG.3

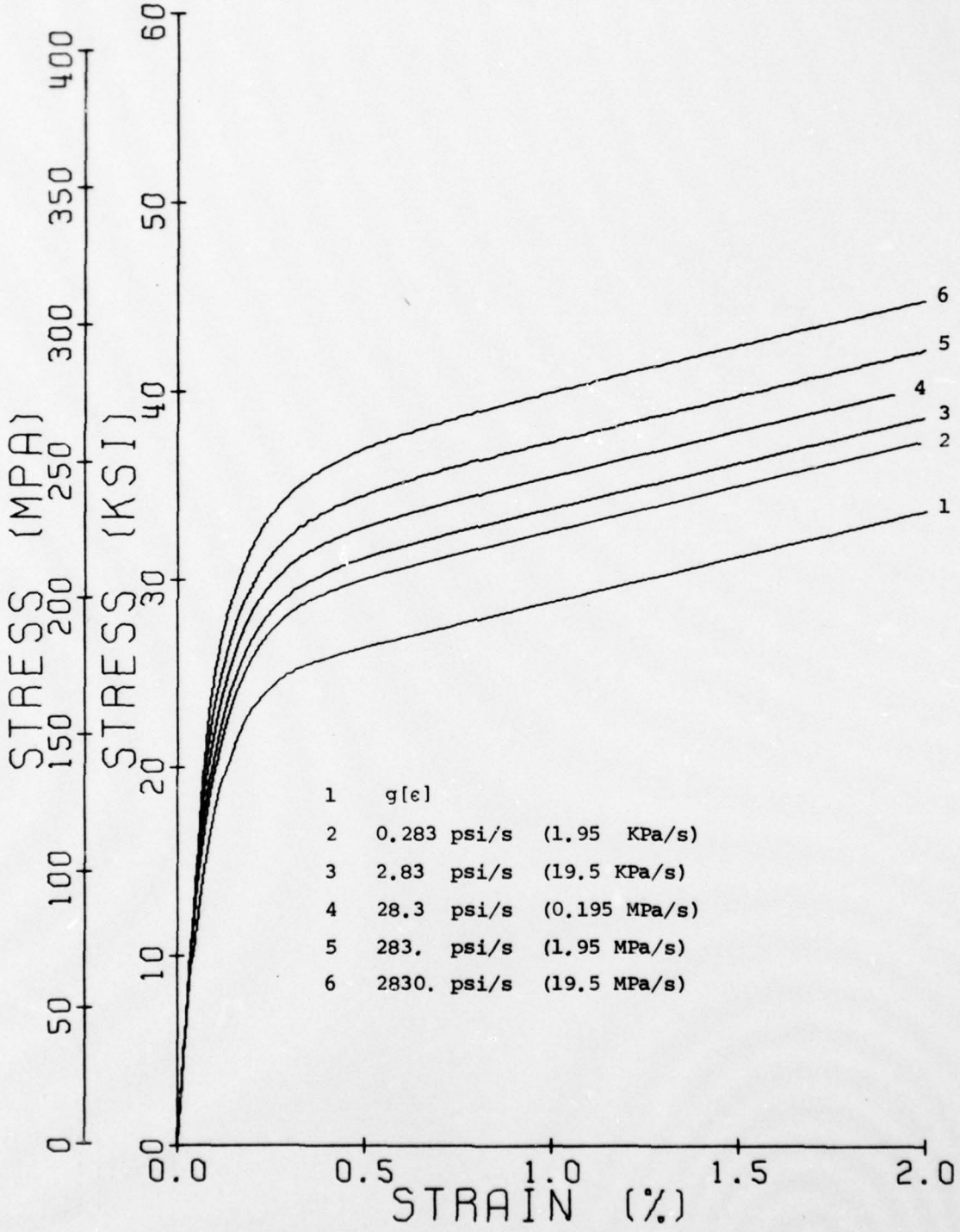
STRESS (MPA)
0
50
100
150
200
250
300
350
400
STRESS (KSI)
0
10
20
30
40
50
60
0.0
0.5
1.0
1.5
2.0
STRAIN (%)
1
2
3
4
5
6
1 g[ε]
2 0.283 psi/s (1.95 KPa/s)
3 2.83 psi/s (19.5 KPa/s)
4 28.3 psi/s (0.195 MPa/s)
5 283. psi/s (1.95 MPa/s)
6 2830. psi/s (19.5 MPa/s)

FIG.4

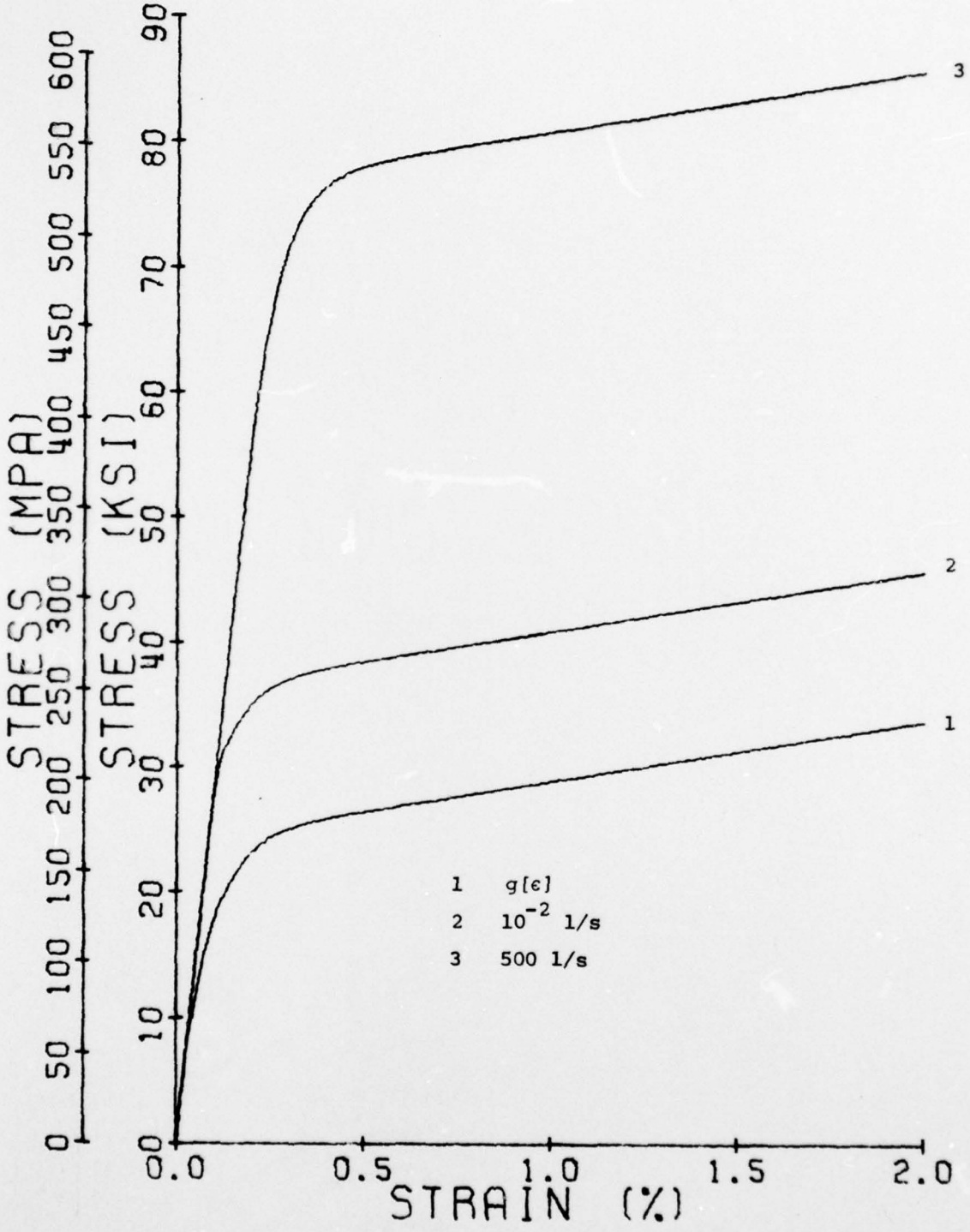
STRESS (MPA)
0 50 100 150 200 250 300 350 400 450 500 550 600
STRESS (KSI)
0 10 20 30 40 50 60 70 80 90
0.0 0.5 1.0 1.5 2.0
STRAIN (%)
1 g[ε]
2 10^-2 1/s
3 500 1/s
1
2
3

FIG.5

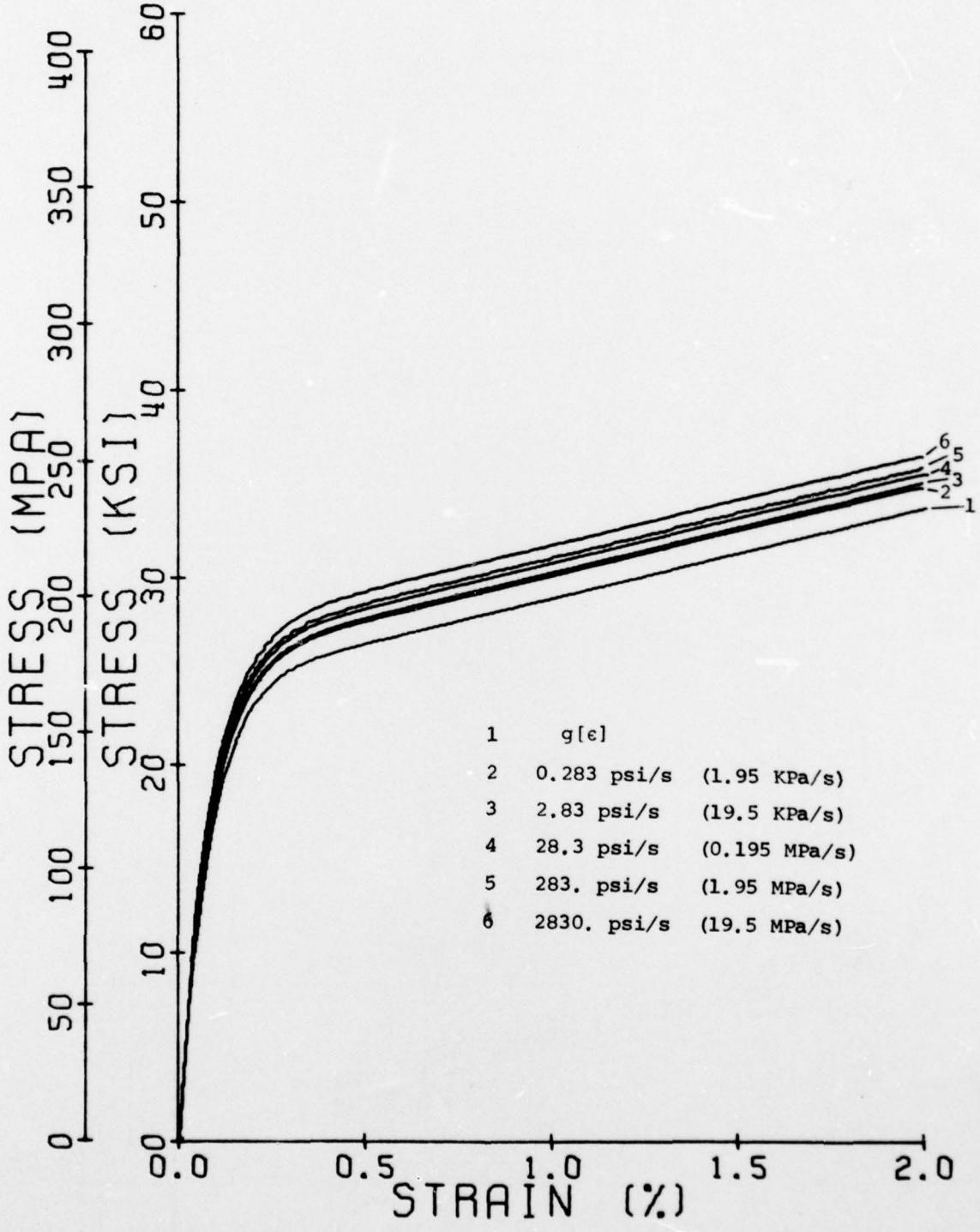
STRESS (MPA)
STRESS (KSI)
0
50
100
150
200
250
300
350
400
0
10
20
30
40
50
60
0.0
0.5
1.0
1.5
2.0
STRAIN (%)
1
2
3
4
5
6
1 g[ε]
2 0.283 psi/s (1.95 KPa/s)
3 2.83 psi/s (19.5 KPa/s)
4 28.3 psi/s (0.195 MPa/s)
5 283. psi/s (1.95 MPa/s)
6 2830. psi/s (19.5 MPa/s)

FIG.6

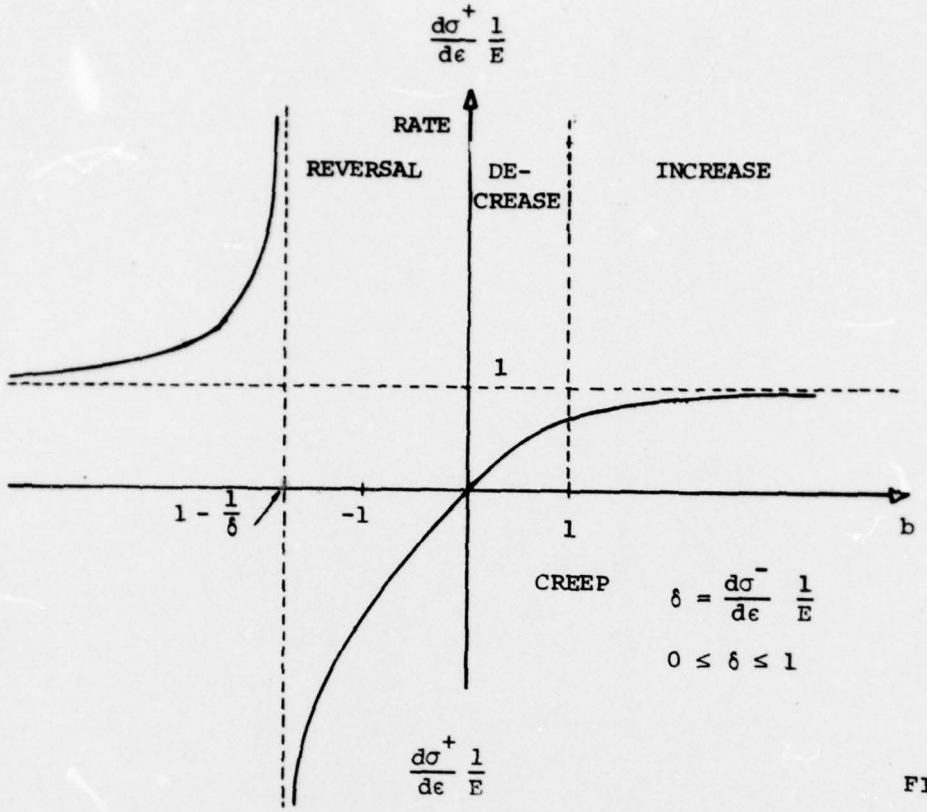
$\frac{d\sigma^+}{d\epsilon}\frac{1}{E}$
RATE
REVERSAL
DE-
CREASE
INCREASE
1
$1-\frac{1}{\delta}$
-1
1
b
CREEP
$\delta = \frac{d\sigma^-}{d\epsilon}\frac{1}{E}$
$0 \le \delta \le 1$
$\frac{d\sigma^+}{d\epsilon}\frac{1}{E}$

FIG. 7a

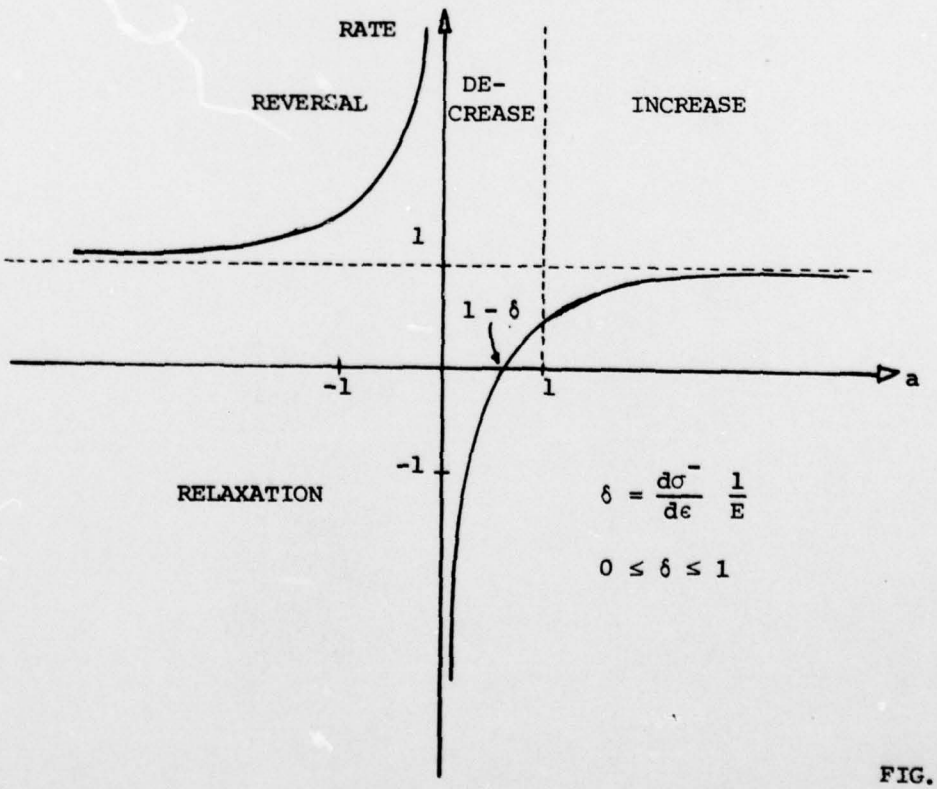
RATE
REVERSAL
DE-
CREASE
INCREASE
1
$1-\delta$
-1
1
a
-1
RELAXATION
$\delta = \frac{d\sigma^-}{d\epsilon}\frac{1}{E}$
$0 \le \delta \le 1$

FIG. 7b

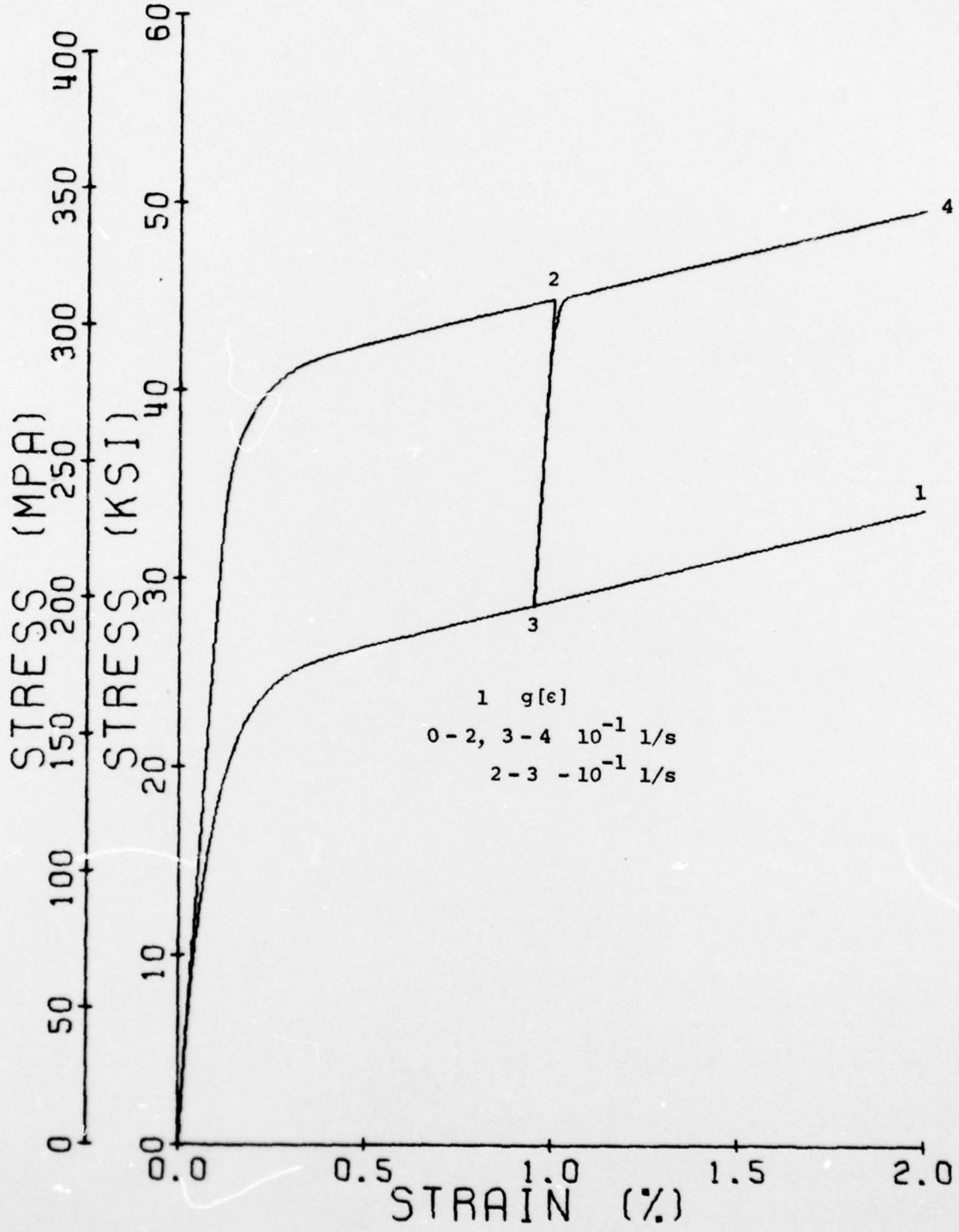
STRESS (MPA)
STRESS (KSI)
0
50
100
150
200
250
300
350
400
0
10
20
30
40
50
60
0.0
0.5
1.0
1.5
2.0
STRAIN (%)
1
2
3
4
1 g[ε]
0-2, 3-4 10^-1 1/s
2-3 -10^-1 1/s

FIG.8a

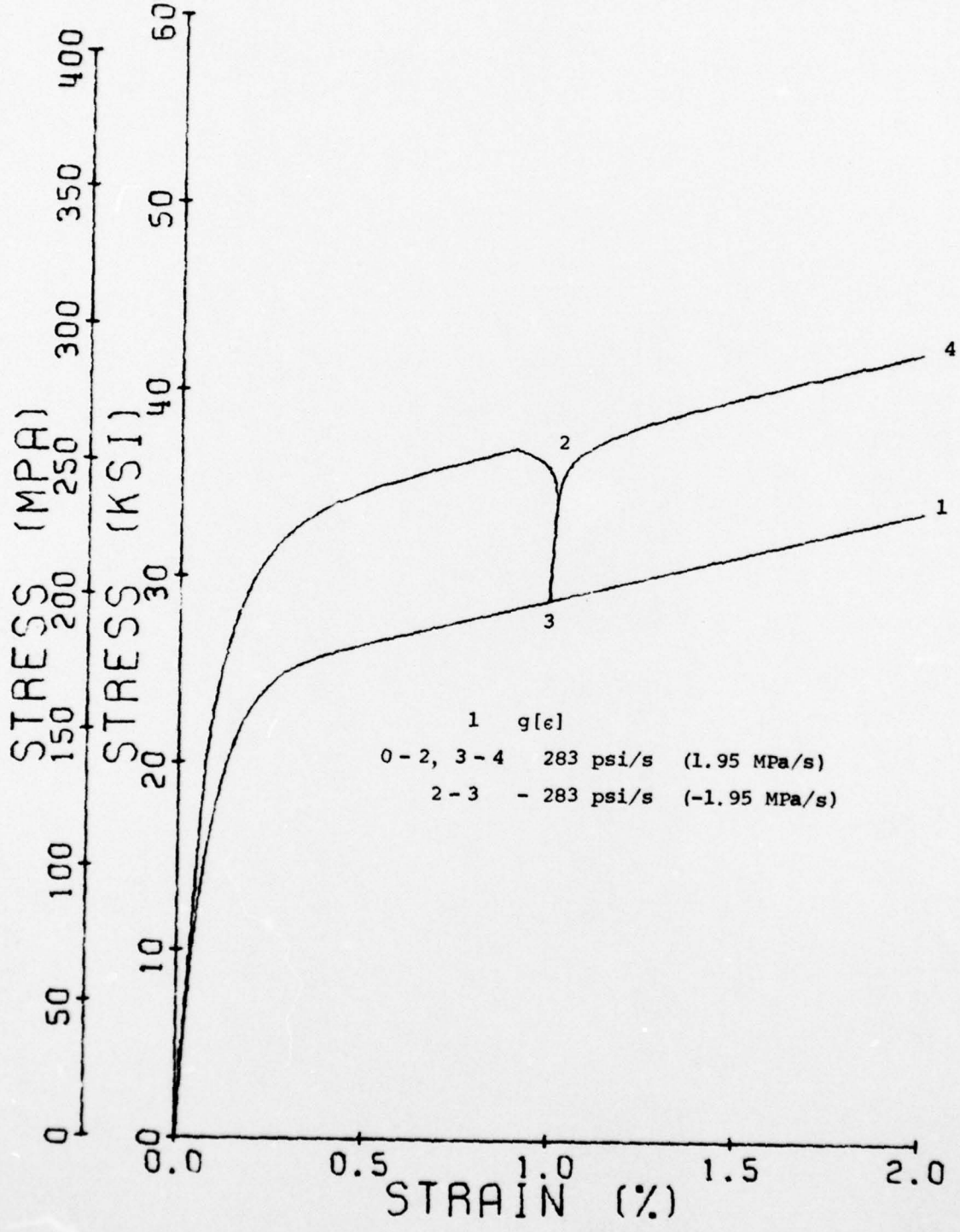
STRESS (MPA)
STRESS (KSI)
0
50
100
150
200
250
300
350
400
0
10
20
30
40
50
60
0.0
0.5
1.0
1.5
2.0
STRAIN (%)
1
2
3
4
1 g[ε]
0 - 2, 3 - 4 283 psi/s (1.95 MPa/s)
2 - 3 - 283 psi/s (-1.95 MPa/s)

FIG.8b


STRESS (MPA)
0
50
100
150
200
250
300
350
400
STRESS (KSI)
0
10
20
30
40
50
60
0.0
0.5
1.0
1.5
2.0
STRAIN (%)
1
2
3
4
5
1 g[ε]
0-2, 3-4 10^-5 1/s
2-3, 4-5 10^-3 1/s

FIG. 9a

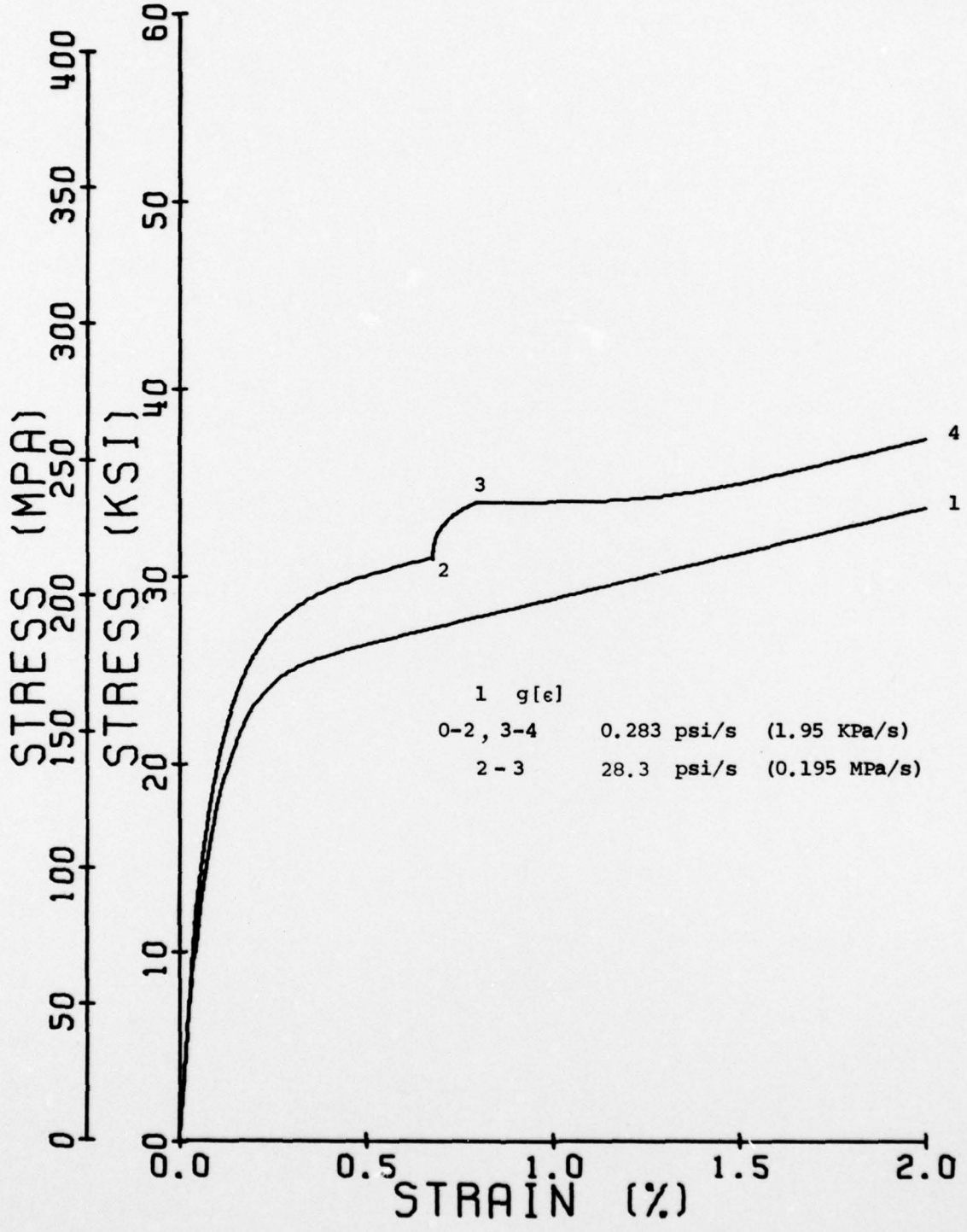
STRESS (MPA)
STRESS (KSI)
0
50
100
150
200
250
300
350
400
0
10
20
30
40
50
60
0.0
0.5
1.0
1.5
2.0
STRAIN (%)
1
2
3
4
1 g[ε]
0-2, 3-4 0.283 psi/s (1.95 KPa/s)
2-3 28.3 psi/s (0.195 MPa/s)

FIG. 9b

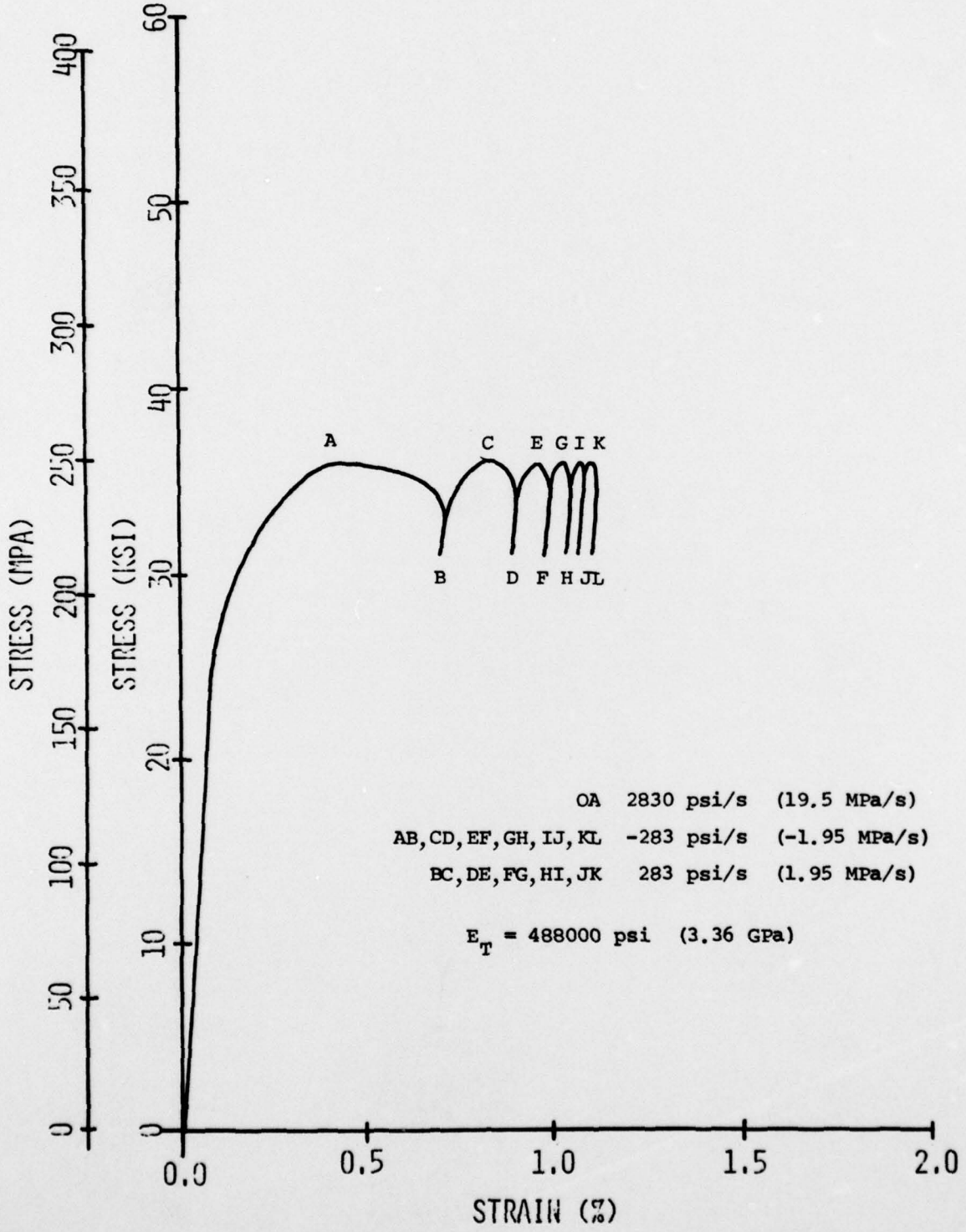
STRESS (MPA)
0
50
100
150
200
250
300
350
400
STRESS (KSI)
0
10
20
30
40
50
60
A
B
C
D
E
F
G
H
I
J
K
L
0.0
0.5
1.0
1.5
2.0
STRAIN (%)
OA 2830 psi/s (19.5 MPa/s)
AB, CD, EF, GH, IJ, KL -283 psi/s (-1.95 MPa/s)
BC, DE, FG, HI, JK 283 psi/s (1.95 MPa/s)
E_T = 488000 psi (3.36 GPa)

FIG.10a

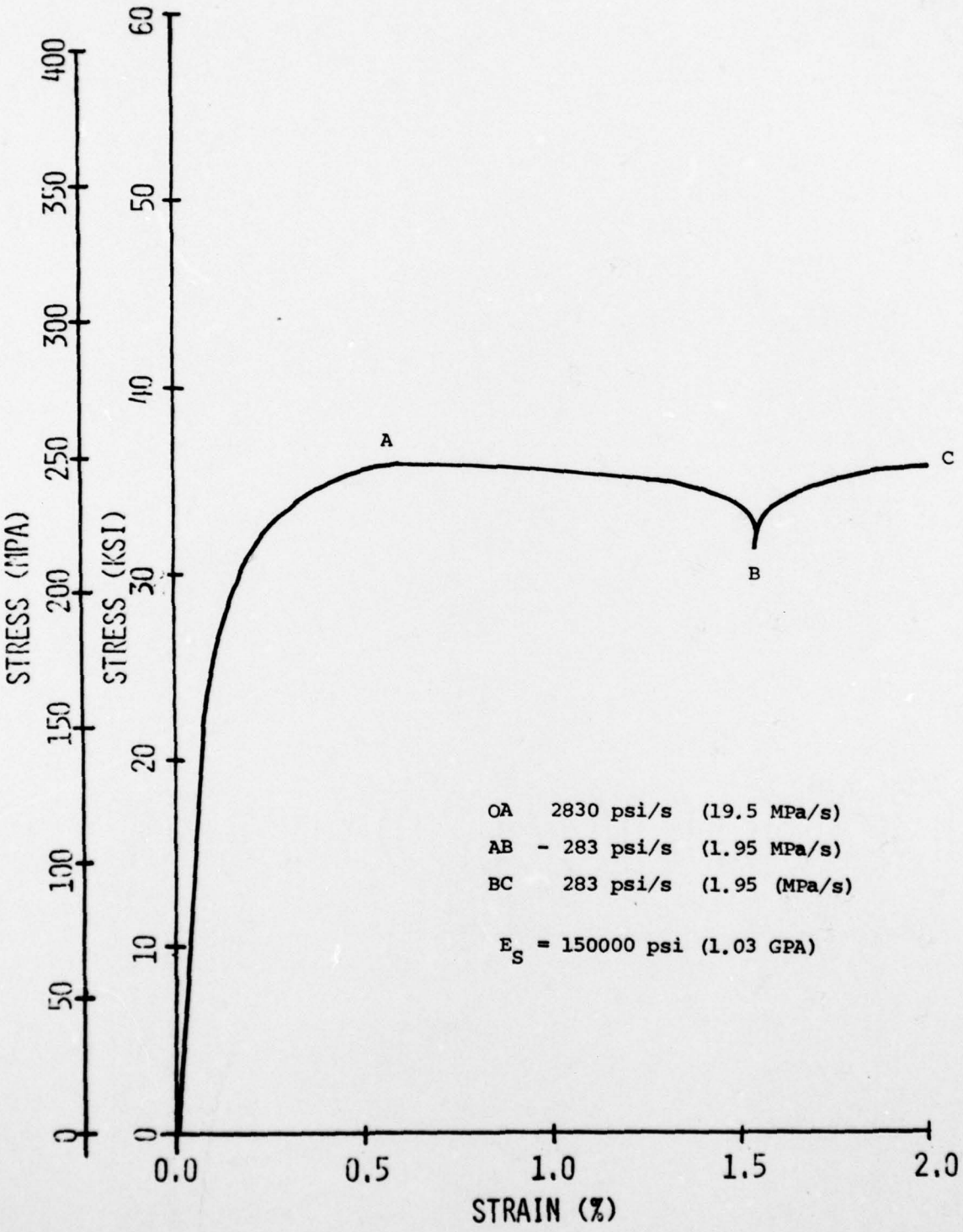
STRESS (MPA)
STRESS (KSI)
0
50
100
150
200
250
300
350
400
0
10
20
30
40
50
60
A
B
C
0.0
0.5
1.0
1.5
2.0
STRAIN (%)
OA 2830 psi/s (19.5 MPa/s)
AB - 283 psi/s (1.95 MPa/s)
BC 283 psi/s (1.95 (MPa/s)
E_S = 150000 psi (1.03 GPA)

FIG. 10b

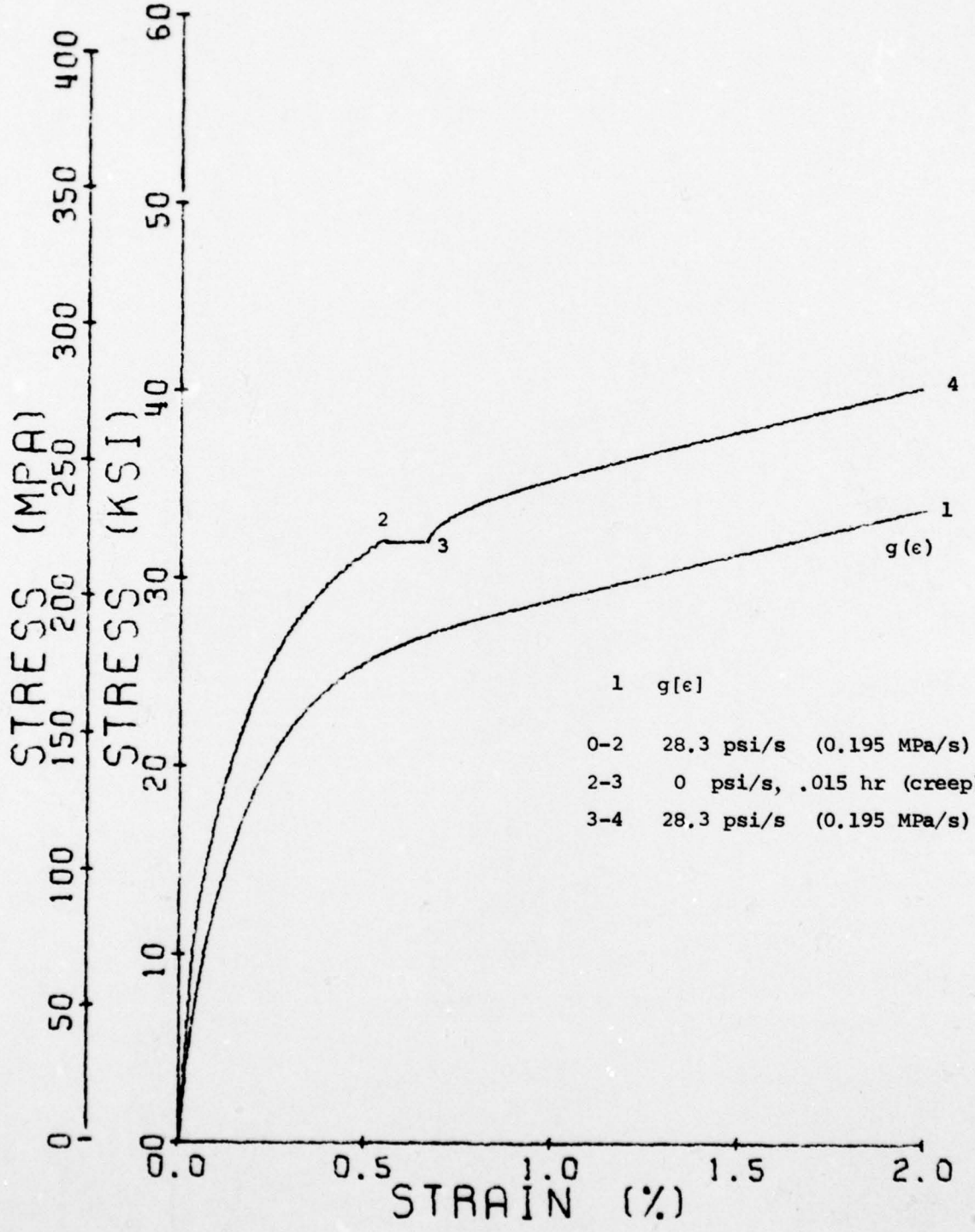
STRESS (MPA)
STRESS (KSI)
0
50
100
150
200
250
300
350
400
0
10
20
30
40
50
60
0.0
0.5
1.0
1.5
2.0
STRAIN (%)
1
2
3
4
g(ε)
1 g[ε]
0-2 28.3 psi/s (0.195 MPa/s)
2-3 0 psi/s, .015 hr (creep)
3-4 28.3 psi/s (0.195 MPa/s)

FIG. 11a

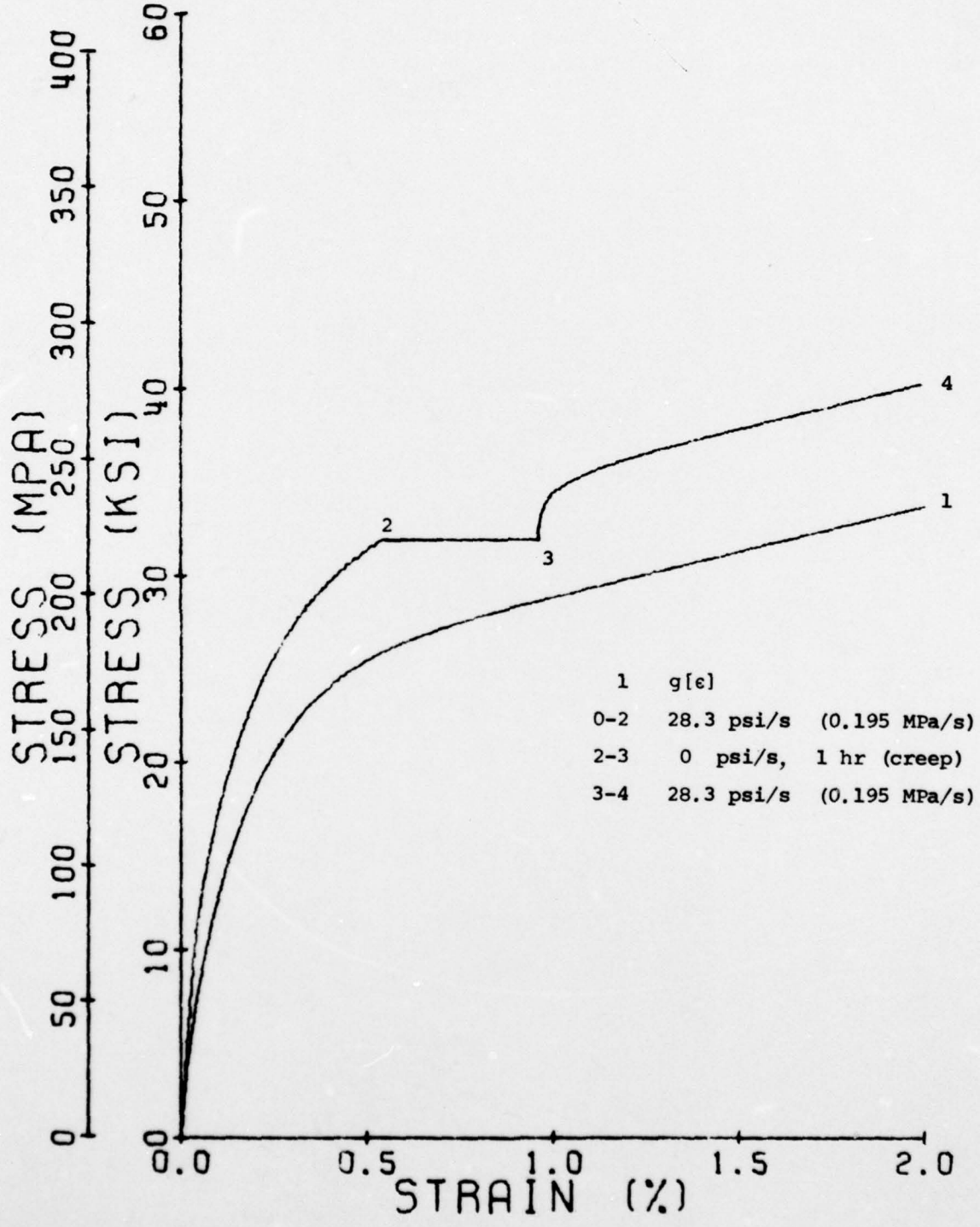
STRESS (MPA)
STRESS (KSI)
0
50
100
150
200
250
300
350
400
0
10
20
30
40
50
60
0.0
0.5
1.0
1.5
2.0
STRAIN (%)
1
2
3
4
1 g[ε]
0-2 28.3 psi/s (0.195 MPa/s)
2-3 0 psi/s, 1 hr (creep)
3-4 28.3 psi/s (0.195 MPa/s)

FIG. 11b

Unclassified

SECURITY CLASSIFICATION OF THIS PAGE *(When Data Entered)*

REPORT DOCUMENTATION PAGE

READ INSTRUCTIONS BEFORE COMPLETING FORM

1. REPORT NUMBER: RPI-CS-78-4	2. GOVT ACCESSION NO.
3. RECIPIENT'S CATALOG NUMBER	
4. TITLE (and Subtitle): Uniaxial Viscoplasticity Based on Total Strain and Overstress	5. TYPE OF REPORT & PERIOD COVERED: Topical Report
6. PERFORMING ORG. REPORT NUMBER	
7. AUTHOR(s): M.C.M. Liu [redacted] E. Krempl	8. CONTRACT OR GRANT NUMBER(s): N00014-76-C-0231
9. PERFORMING ORGANIZATION NAME AND ADDRESS: Department of Mechanical Engineering, Aeronautical Engineering & Mechanics, Rensselaer Polytechnic Institute, Troy, NY 12181	10. PROGRAM ELEMENT, PROJECT, TASK AREA & WORK UNIT NUMBERS: NR 064-571
11. CONTROLLING OFFICE NAME AND ADDRESS: Dept. of the Navy, Office of Naval Research, Structural Mechanics Program, Arlington, VA 22217	12. REPORT DATE: July [redacted]78 13. NUMBER OF PAGES
14. MONITORING AGENCY NAME & ADDRESS *(if different from Controlling Office)*: Office of Naval Research - Resident Representative, 715 Broadway - 5th Floor, New York, NY 10003	15. SECURITY CLASS. *(of this report)*: Unclassified 15a. DECLASSIFICATION/DOWNGRADING SCHEDULE

16. DISTRIBUTION STATEMENT *(of this Report)*

Approved for public release; distribution unlimited

17. DISTRIBUTION STATEMENT *(of the abstract entered in Block 20, if different from Report)*

18. SUPPLEMENTARY NOTES

19. KEY WORDS *(Continue on reverse side if necessary and identify by block number)*

Viscoplasticity, creep, relaxation, rate-effects, stress-strain experiments, strain-rate history effects

20. ABSTRACT *(Continue on reverse side if necessary and identify by block number)*

A previously proposed uniaxial constitutive equation nonlinear in the Cauchy stress and the engineering strain but linear in the stress and strain rates is specialized to an overstress model. Two unknown coefficient functions are determined by extrapolation of room temperature relaxation data on Type 304 stainless steel. The stiff first-order nonlinear differential equations are then numerically integrated for a variety of test histories. These include: strain control with strain rates from 10^{-6} s^{-1} to 500 s^{-1}; stress control with

DD FORM 1 JAN 73 1473 EDITION OF 1 NOV 65 IS OBSOLETE

S/N 0102-LF-014-6601

Unclassified

SECURITY CLASSIFICATION OF THIS PAGE *(When Data Entered)*

409 359

stress rates from 1.95 KPa s^{-1} to 19.5 MPa s^{-1}; instantaneous large changes in strain rate (strain-rate history effects) and stress rate; partial unloading and reloading in strain and stress control and tension-tension cyclic creep. The computed results show good qualitative agreement with tests. Based on these results we consider the model a good representation of metal deformation behavior as long as the overstress does not change sign.